RM No. E7K19

CASE FILE
COPY

NACA

RESEARCH MEMORANDUM

PRELIMINARY INVESTIGATION OF CONE-TYPE DIFFUSERS DESIGNED FOR MINIMUM SPILLAGE AT INLET

By Roger W. Luidens and Henry Hunczak

Flight Propulsion Research Laboratory
Cleveland, Ohio

NATIONAL ADVISORY COMMITTEE
FOR AERONAUTICS

WASHINGTON

May 3, 1948
Declassified June 11, 1953

NATIONAL ADVISORY COMMITTEE FOR AERONAUTICS

RESEARCH MEMORANDUM

PRELIMINARY INVESTIGATION OF CONE-TYPE DIFFUSERS DESIGNED FOR MINIMUM SPILLAGE AT INLET

By Roger W. Luidens and Henry Hunczak

SUMMARY

A preliminary investigation of cone-type diffusers designed for minimum spillage at the inlet during operation was conducted in the NACA Cleveland 18- by 18-inch supersonic tunnel at a Mach number of 1.85. This design dictates that the oblique shock fall at or within the inlet and that the normal shock be within the diffuser at design conditions.

The pressure recoveries of a series of stationary cones with included angles of 20°, 30°, 40°, 50°, and 60° were investigated. The 30° stationary-cone configuration with a throat length of 0.29 inlet diameters gave a pressure recovery of 0.859 at an angle of attack of 0° and 0.838 at 5°. The 30° cone configuration investigated with various throat lengths showed an increase in pressure recovery from 0.859 to 0.869 as the throat length was increased to 0.46 inlet diameters.

An investigation of the pressure recovery of movable-cone configurations, or variable-contraction-ratio diffusers, as a function of the contraction ratio disclosed that the maximum total contraction ratio that could be attained before choking at the throat occurred was 1.351 as compared with the theoretical isentropic value of 1.495. A maximum pressure recovery of 0.891 was attained at this contraction ratio. Perforations added at the throat of the diffuser to accomplish partial boundary-layer removal and aid in normal-shock stabilization allowed the maximum total contraction ratio to be increased to 1.384 and raised the pressure recovery to 0.933.

INTRODUCTION

Operation of ram-jet engines at supersonic speeds requires that the diffuser efficiently convert the kinetic energy of the air stream to pressure energy at the combustion chamber with a minimum of external drag. The diffuser should, moreover, perform

as efficiently as possible at other than design conditions. The optimum diffuser design therefore incorporates a compromise between the factors of drag and pressure recovery over a range of operation. A number of pressure-recovery investigations representing various compromises between the aforementioned factors have been conducted but without drag measurements. The diffuser representing optimum performance therefore cannot as yet be chosen.

A contributing factor to the drag of a ram jet, however, is the additive drag (reference 1), which results directly from flow spillage at the inlet. Flow spillage is defined as the mass flow in a free-stream tube having a diameter equal to the inlet diameter minus the mass flow that enters the diffuser. The additive drag may be calculated by integration of the momentum equation about the ram jet.

The performance of convergent-divergent diffusers with all deceleration internal is discussed in references 2 and 3. This type of diffuser is designed with the maximum total contraction ratio that will allow the normal shock to enter the diffuser so that supersonic flow may be established in the inlet. By this design criterion, however, the velocity at the throat of the diffuser is considerably above sonic and a normal shock located at the throat still results in a large total-pressure loss. The convergent-divergent diffuser can operate through a range of flight Mach numbers about the design Mach number once the flow pattern has been established, and there is no additive drag in this range of operation because there is no flow spillage. If for any reason the back pressure on the diffuser (the pressure in the combustion chamber) becomes greater than the pressure that the diffuser can attain, the normal shock is forced from the throat of the diffuser to a position ahead of the diffuser with a loss in pressure recovery, a decrease in mass flow, and an increase in drag.

Projecting-cone diffusers with all supersonic deceleration external are described in reference 1. This type of diffuser operates with the normal shock ahead of or at the diffuser inlet and is therefore subject to no starting limitations and no discontinuities in flow configuration. The highest pressure recoveries for this type of design occur when the air that has been efficiently decelerated near the cone surface enters the diffuser and the less-compressed air farther from the cone surface is spilled around the diffuser.

Diffusers that combine internal and external contraction are reported in references 4 to 7. In general, the highest pressure recoveries are reported for the flow configurations that indicate considerable flow spillage.

A preliminary investigation of cone-type diffusers designed for minimum spillage at the inlet during operation was therefore conducted in the NACA Cleveland 18- by 18-inch supersonic wind tunnel. The first part of this report concerns the investigation of the pressure recoveries that may be expected from stationary-cone configurations when an additive drag (as judged from the external flow pattern) and an inlet area corresponding to a convergent-divergent diffuser of the same mass flow are maintained. At design conditions the normal shock is thus within the diffuser and the oblique shock generated by the projecting cone must fall at the lip of the inlet. These diffusers combine internal and external deceleration, the internal contraction being limited by the conditions that permit entrance of the normal shock. Added effects of the design stipulations are facilitating accurate determination of the mass rate of flow and minimizing interaction of the internal and external aerodynamics of the diffuser.

The second part of the report covers an investigation of the pressure recoveries that can be obtained with a movable-cone, or variable-contraction-ratio, diffuser which, although it has internal contraction, is not subject to starting limitations. The contraction ratio of the diffuser can be reduced to allow the normal shock to enter the diffuser and then increased to permit maximum deceleration of the flow before the transition from supersonic flow to subsonic flow occurs. In this manner high theoretical pressure recoveries are attainable without increases in the external drag.

SYMBOLS

The following symbols are used in this report and are shown in figures 1 and 2(a):

A	area
D	inlet diameter
d	maximum diameter of cone
L	throat length
l	length of supersonic inlet
M	Mach number
P	total pressure
s	length of support fairing

α angle of attack

δ deflection angle of flow through oblique shock standing at angle φ

γ ratio of specific heats

φ shock angle

θ cone angle

ω angle formed between axis of symmetry and line joining tip of cone and lip of inlet

Subscripts:

0 free stream

1 immediately behind oblique shock

2 minimum-flow area, or diffuser throat

3 immediately behind normal shock

4 exit of simulated combustion chamber

e entrance of diffuser defined along imaginary surface perpendicular to cone surface from line of intersection of oblique shock and inlet

c cone surface

cr critical

max maximum

APPARATUS AND PROCEDURE

Cone-type diffusers designed for minimum spillage at the inlet were investigated in the Cleveland 18- by 18-inch supersonic tunnel at a Mach number of 1.85. The tunnel was calibrated by measuring the oblique shock generated by a cone and the total pressure behind a normal shock. The absolute values of tunnel total pressure and Mach number determined by these methods are accurate to about 2 percent. The precision in measuring the diffuser total-pressure recovery was ± 0.5 percent.

The experimental investigation was divided into two parts. The diffusers first investigated have stationary cones of various cone angles and contraction ratios. Cylindrical inlets were used with these configurations. The following table gives the cone, throat, and inlet combinations (see fig. 2(a)):

Cone angle θ (deg)	Throat length L (in.)	Throat-inlet ratio L/D	Shock-position parameter ω/φ	Inlet length l (in.)	Maximum cone diameter d (in.)	Support-fairing length s (in.)
20	0.64	0.29	1.00	2.36	0.946	0.662
30	.64	.29	1.00	2.36	1.028	1.286
40	0	0	1.15	2.36	1.113	1.814
40	.20	.09	1.00	2.36	1.113	1.814
50	.38	.17	1.00	2.36	1.120	1.885
60	.90	.41	1.00	2.36	1.080	1.355
30	1.00	.46	1.15	2.92	1.028	1.286
30	2.00	.91	1.15	3.92	1.028	1.286

The stationary cones were mounted on a central body supported in the subsonic diffuser by four biconvex struts having a thickness ratio of 13 percent of the chord (fig. 2(a)).

The diffusers studied in the second part of the investigation have a movable 30° cone for varying the contraction ratio and two inlets that could be mounted interchangeably on the subsonic diffuser (fig. 2(b)). The two inlets differed in internal geometry, inlet 2 being designed to give a more uniform and gradual subsonic diffusion than inlet 1. The external shape of the diffusers was arbitrarily chosen for ease in construction. The large angle of the lip could be greatly reduced to give low drags for practical applications.

For further investigation, 29 holes were drilled perpendicular to the external surface of inlet 2 with a No. 38 drill (0.101-in. diameter). The holes were arranged in two staggered rings 1 and $1\frac{1}{8}$ inches downstream of the inlet entrance. A ring of 15 additional holes was later added $1\frac{3}{16}$ inches downstream of the inlet entrance.

The cone was mounted on a mechanism that gave it an axial movement of approximately 0.85 inch. The total contraction ratios for the configuration of inlets 1 and 2 could thus be varied from

1.060 to 1.500 and 1.131 to 1.800, respectively. Contraction ratios were determined as a function of tip projection of the cone. The tip projection was measured with a cathetometer. Repeated trials established the precision of measuring tip projection as ±0.01 inch, giving a possible error of ±0.005 in the determination of the contraction ratio.

The subsonic diffuser used for the movable-cone configurations is shown in figure 2(b). A central body containing the cone-return mechanism was mounted on four streamlined struts (having a thickness ratio of 9.5 percent) in the diverging part of the diffuser and extended forward to the rear fairing of the cone. When the movable-cone diffusers were investigated, the cone was retracted until the contraction ratio was such that the normal shock entered the diffuser (reference 2). In order to determine the maximum total contraction ratio A_0/A_2 for a configuration, the cone was then moved forward until the flow choked. The maximum pressure recovery was then obtained when the normal shock was positioned near the throat of the diffuser by controlling the outlet area.

All diffuser combinations were mounted on a simulated combustion chamber having a variable outlet area controlled by means of a conical damper (fig. 2(c)). The pressure recovery at the simulated combustion chamber was measured with a pitot-static rake. Pressures were measured on a multiple-tube mercury-manometer board and photographically recorded. The air flow about the inlet was visually observed with a two-mirror schlieren system to establish whether spillage occurred.

The total pressure of the free stream at the diffuser inlets was calculated from the total pressure measured in the tunnel settling chamber for each run and the ratio of free-stream total pressure to settling-chamber pressure as determined from previous tunnel calibrations. Ambient conditions of total temperature and dew point were essentially constant.

DISCUSSION AND RESULTS

The total-pressure recovery P_4/P_0 of the stationary-cone diffusers is presented as a function of the following variables: cone angle θ, outlet-inlet area ratio A_4/A_0, angle of attack α, and throat length L, expressed in inlet diameters L/D. The total contraction ratio A_0/A_2 and the internal contraction ratio A_e/A_2 were predetermined by the design. The total-pressure recovery of the movable-cone configuration was considered a function of the

total contraction ratio A_0/A_2, the outlet-inlet air ratio A_4/A_0, and the angle of attack α. The effect of stabilizing the normal shock at the throat of the diffuser by means of perforations, as suggested in reference 8, is also discussed.

Pressure Recovery with Stationary Cones

The optimum condition of each configuration was designed for a free-stream Mach number of 1.85 from the following considerations: The tip projection was chosen to allow a minimum flow spillage at the design operating conditions and a maximum flow spillage for starting the diffuser. These requirements are satisfied when the oblique shock falls at the lip of the inlet ($\omega/\varphi = 1$). The maximum internal contraction ratio that would then allow the normal shock to enter was calculated by assuming the Mach number at station e equal to the Mach number at the cone surface, station c. Although this assumption gives a conservative value for the diameter of the central body, it was expedient because the entrance of the normal shock was essential to the investigation. The values of the internal contraction ratio A_e/A_2 and the corresponding total contraction ratio A_0/A_2 thus computed are shown in figure 3 as a function of the cone angle θ. For $\theta > 47^\circ$ the contraction ratios are only a good approximation, as the detached bow wave formed ahead of the lip of the inlet decreases the size of the entering stream tube.

Variation with cone angle. - The theoretical curve of the variation of maximum total-pressure recovery $(P_4/P_0)_{max}$ with cone angle θ shown in figure 4 was calculated at the design conditions by the approximate method outlined in reference 6, that is, assuming $M_e = \frac{M_1 + M_c}{2}$ and neglecting subsonic diffuser losses as well as the effects of the internal oblique shock originating at the lip of the cylindrical inlet. For $\omega/\varphi = 1$ the normal shock was assumed to occur at station e for the normal shock at the entrance of the diffuser or at station 2 for the normal shock within the diffuser. The Mach number at station 2 was determined from the Mach number at station e and the internal contraction ratio. The total-pressure recovery was determined as the product of the pressure recoveries across the oblique and normal shocks.

The solid curve of figure 4 is the maximum theoretical pressure recovery with the normal shock at the throat of the diffuser and the dashed curve is the maximum theoretical pressure recovery

with the normal shock at the entrance of the diffuser. The upper curve does not exist for $\theta > 47^\circ$ because the normal shock can no longer enter the diffuser. At the lip of the inlet the flow must be parallel to the interior of the inlet, which for this investigation is cylindrical with its axis parallel to the free-stream direction at zero angle of attack. The flow immediately downstream of the oblique shock, however, is deflected outward at an angle δ, with a corresponding reduction in the local Mach number. If the flow is then to follow the interior of the inlet, it must be turned a second time through the angle δ but at the reduced Mach number. For an elemental area, these flow turnings are essentially two-dimensional, and a limiting turning angle exists, which if exceeded forms a detached bow wave. This phenomenon occurs at the lip of the inlet for $\theta > 47^\circ$ at a free-stream Mach number of 1.85. The solid curve with a discontinuity at $\theta = 47^\circ$ then represents the maximum theoretical pressure recoveries for this investigation.

The data points of maximum total-pressure recovery are also plotted against cone angle in figure 4. The theoretical discontinuity at $\theta = 47^\circ$ was experimentally indicated between cone angles of 40° and 50° by the fact that the normal shock entered the diffuser for the 40° cone but did not for the 50° cone. Optimum conditions were expected from the 40° cone configuration. However, the location of the normal shock became unstable at total-pressure recoveries of about 0.81 so that higher pressure recoveries were not obtained with the normal shock within the diffuser.

A schlieren photograph of the 50° cone (fig. 5(a)) shows the appearance of the shock at the inlet for outlet conditions that would allow entrance of the normal shock except for the excessive turning angle previously discussed. What appears to be a shock normal to the free stream in figure 5(a) is actually the three-dimensional projection of the bow shock ahead of the inlet lip. The low pressure recovery is caused by reacceleration of the flow downstream of the throat and a strong shock in the subsonic part of the diffuser. The second photograph of the 50° cone (fig. 5(b)) shows the flow configuration for a maximum total-pressure recovery of 0.879. The normal shock is ahead of the inlet and this configuration is subject to additive drags.

The 40° cone photograph (fig. 5(c)) shows the condition where the normal shock is within the diffuser and no bow shock has formed at the lip of the diffuser. (The shock disturbances along the inlet are caused by the instrumentation shown in other photographs of fig. 5 but rotated through 45° in this picture.)

With the 30° cone (L/D = 0.46), the shock configuration was similar to that shown in figure 5(d), and a maximum total-pressure recovery of 0.869 (fig. 4) was attained. The normal shock was within the diffuser and the oblique shock was at the lip of the inlet; this configuration is therefore considered optimum for the investigation.

The limiting cone angle that causes a bow wave to form at the lip of the inlet is shown in figure 6 as a function of the design Mach number. In general, the cone angle to give optimum conditions as defined for this investigation is less than the limiting cone angle but is not clearly determined because curves showing the variation of maximum pressure recovery with cone angle are flat at the optimum conditions, as may be seen from figure 4. (See also reference 6.) For this reason, a range of cone angles less than the limiting cone angle will yield pressure recoveries close to the optimum pressure recovery for this type of configuration.

The total-pressure recovery representing optimum conditions for the cones investigated was 0.869 ($\theta = 30°$, L/D = 0.46). For comparison with other types of diffuser investigated at the same Mach number, the total-pressure recovery of the convergent-divergent diffuser as given in reference 3 was 0.838. The total-pressure recovery of a single-shock projecting-cone diffuser when all supersonic compression is external is given in reference 6 as 0.922.

Variation with outlet-inlet area ratio. - The theoretical curves of figure 7 were developed in reference 3 by assuming no mass spillage at the inlet, adiabatic flow through the diffuser, and negligible boundary-layer effects at the exit area. The general equation relating the pressure recovery and the outlet-inlet area ratio under these assumptions may be written as

$$\frac{P_4 A_4}{P_0 A_0} = \frac{M_0}{M_4}\left(\frac{1 + \frac{\gamma-1}{2} M_4^2}{1 + \frac{\gamma-1}{2} M_0^2}\right)^{\frac{\gamma+1}{2(\gamma-1)}}$$

In general, the flow at the exit of the test apparatus is choked so that $M_4 = 1$; then at a free-stream Mach number M_0 of 1.85 and a ratio of specific heats γ of 1.40, the equation reduces to

$$\frac{P_4 A_4}{P_0 A_0} = 0.669$$

which gives the relation between outlet-inlet area ratio and pressure recovery up to the maximum pressure recovery. The maximum pressure recovery for this equation is the value determined in the section entitled "Variation with cone angle" if subsonic-diffuser losses are neglected.

In general, the theory and the experimental results correspond in the manner indicated by previous investigations (references 6 and 7). The experimental-data points fall to the right of the theoretical curves because of the restriction of the exit area by boundary layer on the exit cone and the interior of the diffuser. The discrepancies between the peak experimental recoveries and the theoretically predicted values may be attributed to subsonic-diffuser losses and the instability of the normal shock in the vicinity of the throat of the diffuser. Discontinuities were expected in the pressure recovery for those configurations with $\theta < 47^\circ$ as the normal shock moved from a position near the throat of the diffuser to the entrance of the diffuser. (See fig. 4.) However, because of the instability of the normal shock near the throat of the diffuser, these discontinuities were not observed for the 30° and 40° cones, as may be seen from figures 7(a) and 7(b).

Variation with angle of attack. - For the stationary-cone configuration, figure 7(a) indicates the effect of angle of attack on the 30° cone $(L/D = 0.29)$ by showing the variation of pressure recovery with outlet-inlet area ratio for angles of attack of 0° and 5°. The maximum total-pressure recovery dropped from 0.859 at an angle of attack of 0° to 0.838 at 5°. Figures 5(d) and 5(e) are schlieren photographs of the flow configuration. Comparison of these figures shows that the oblique shock for the diffuser at an angle of attack of 5° moved only slightly from its position with the diffuser at 0° and that the normal shock is still within the diffuser. From shock theory, the deflection through an oblique shock is dependent only on the free-stream Mach number and the shock angle with respect to the free stream. Because the shock angle did not change appreciably with the angle of attack of the cone, the flow deflection through the shock generated by the cone is relatively independent of small angles of attack. With cone angles close to the limiting cone angle, the increased turning angle at the lip of the inlet with the diffuser at small angles of attack may be expected to form a bow wave ahead of the inlet.

Reference 3 reports a decrease in the total-pressure recovery of a convergent-divergent diffuser from 0.838 at an angle of attack of 0° to 0.764 at 5°. Reference 6 reports a corresponding decrease in total-pressure recovery from 0.922 to 0.908 for a single-shock projecting-cone diffuser.

Variation with throat length. - In the investigation of convergent-divergent diffusers reported in reference 3, a high pressure recovery was found to be dependent essentially on the throat length; and a throat length, expressed in inlet diameters, of $L/D = 1.2$ ($L = 2$ in.) was found to give optimum recovery. The data presented in figure 8 for the type of diffuser investigated herein indicated that increasing the throat length from $L/D = 0.29$ to $L/D = 0.46$ raised the pressure recovery from 0.859 to 0.869.

Pressure Recovery of Movable-Cone Configurations

Variation with contraction ratio. - The theoretical curve of maximum total-pressure recovery $(P_4/P_0)_{max}$ plotted against total contraction ratio A_0/A_4 for the normal shock contained by the diffuser (fig. 9) was obtained by assuming that $M_e = \frac{M_1 + M_c}{2}$ and applying a one-dimensional reduction in Mach number between A_e and A_2. The maximum theoretical total-pressure recovery for a given contraction ratio is again the product of the pressure recovery across the conical shock and the pressure recovery across a normal shock occurring at station 2 for the Mach number at that station. The total-pressure ratio across an oblique shock generated by a 30° cone at a free-stream Mach number of 1.85 is $P_1/P_0 = 0.999$. The total-pressure loss across the reflection of the oblique shock from the interior of the inlet has been neglected. The optimum theoretical pressure recovery occurs when there is no total-pressure loss at the throat of the diffuser corresponding to the transition from supersonic to subsonic flow, and for this condition the total-pressure recovery of the diffuser, neglecting subsonic-diffuser losses, is 0.999. This optimum condition occurs when the total contraction ratio is such that a Mach number of unity exists at the throat. This ratio is also the theoretical maximum contraction ratio that can exist before a normal shock is forced ahead of the diffuser.

For inlet 1, the maximum total-pressure recovery is presented as a function of the total contraction ratio (fig. 9(a)). The maximum total contraction ratio attainable, after supersonic flow was established through the throat of the inlet, before choking at the throat occurred was 1.356 as compared with the theoretical isentropic value of 1.495. Figure 9(a) shows that this contraction ratio also gave the highest total-pressure recovery of 0.874 for inlet 1.

The maximum theoretical contraction ratio is greater than that actually attained. This discrepancy can be attributed in part to the build-up of the boundary layer on the surface of the cone and the inlet, which produced a virtual but unstable throat smaller than the geometric throat area calculated.

For inlet 2 (unperforated), the maximum contraction ratio with the normal shock contained by the diffuser was 1.351, the same as that of inlet 1 within the limits of precision of the measurements. (See APPARATUS AND PROCEDURE section.) The pressure recovery, however, increased to 0.891 (fig. 9(b)). Inlet 2 gave consistently higher recoveries than inlet 1 for contraction ratios greater than 1.230. The improved performance of inlet 2 is attributed in part to the change in geometry to give a more uniform and gradual subsonic diffusion. (See fig. 2(b).)

In order to stabilize the normal shock in the throat of the inlet and relieve the boundary layer, the throat of inlet 2 was perforated (reference 8). The total contraction ratio could be increased to 1.371, by making the area of the perforations 17 percent of the area of the throat (based on the maximum unperforated $A_0/A_2 = 1.351$). The maximum total-pressure recovery was improved to 0.925. A further increase in the area of the perforations to 25.8 percent of the throat area (also based on $A_0/A_2 = 1.351$) increased the total contraction ratio to 1.384 and raised the total-pressure recovery to 0.933. The net improvement in maximum total-pressure recovery due to the perforations was 4.7 percent while the contraction ratio was increased 2.4 percent. This increase in the total contraction ratio indicates a partial removal of the boundary layer. The improvement of the maximum pressure recovery for contraction ratios greater than 1.320 (fig. 9(b)) indicates that better stabilization of the normal shock in the diffuser was achieved.

Variation with outlet-inlet area ratio. - The variation of total-pressure recovery P_4/P_0 with outlet-inlet area ratio A_0/A_2 is shown in figure 10 for two possible shock configurations. With the normal shock inside the diffuser, the theoretical curve is given by the equation $(P_4/P_0)(A_4/A_0) = 0.669$ and is shown in figure 10 as a solid line. The dashed curve corresponds to the condition when subsonic flow is entering the inlet and flow spillage exists. This curve was derived from one-dimensional relations with the assumption that the flow first undergoes a total-pressure loss through a normal shock at the free-stream Mach number. The equation for the curve is

$$\frac{P_4 A_4}{P_0 A_0} = M_0 \left(\frac{1 + \frac{\gamma-1}{2}}{1 + \frac{\gamma-1}{2} M_0^2} \right)^{\frac{\gamma+1}{2(\gamma-1)}} \left(\frac{A_0}{A_2} \right)_{cr} \left(\frac{A_2}{A_0} \right)$$

where $(A_0/A_2)_{cr}$ is the maximum contraction ratio at which the diffuser will start without choking at the throat (reference 2). The factor $(A_0/A_2)_{cr}(A_2/A_0)$ is the ratio of the mass flow passing through the diffuser when spillage occurs at the inlet to the mass flow through the diffuser without spillage at the inlet.

For the conditions shown in figure 10(a), the normal shock that must be contained by the diffuser for optimum recovery cannot reenter the diffuser once it has been forced outside the diffuser. The result is a lowering of the pressure recovery as well as a loss of mass flow through the diffuser. From the theoretical equation, it is apparent that the amount of flow spillage is a function of the total contraction ratio for a given Mach number. Figures 10(b) and 10(c) show that the actual operation of the diffuser follows the theoretical trends and that the maximum total contraction ratio at which the normal shock could reenter was 1.180, which corresponds to the theoretical value of 1.181 (reference 2). Schlieren photographs of inlet 2 for supersonic flow into the inlet and no spillage, and for subsonic flow into the inlet with spillage, are shown in figures 11(a) and 11(b). The visible flow patterns were the same for inlet 1; photographs of inlet 2 were chosen for presentation because of the quality of the pictures.

Variation with angle of attack. - At an angle of attack of 5° with the normal shock near the throat of the diffuser, a vibration of the cone of approximately 1/4-inch amplitude was observed, which did not occur at an angle of attack of 0°. As a result, reliable pressure-recovery data could not be obtained. With the normal shock positioned well downstream of the throat, there was no vibration of the cone and the maximum total contraction ratio that could be attained before choking occurred at the throat was 1.244. The schlieren photographs of inlet 1 at an angle of attack of 5° shown in figures 11(c) and 11(d) illustrate the asymmetrical flow pattern with supersonic and subsonic flow into the inlet.

SUMMARY OF RESULTS

An investigation of cone-type diffusers designed for minimum spillage at the inlet at a Mach number of 1.85 gave the following results:

1. The 30° stationary-cone configuration with a throat length of 0.29 inlet diameter gave a total-pressure recovery of 0.859 at an angle of attack of 0° and 0.838 at 5°. At an angle of 0° increasing the throat length to 0.46 inlet diameters improved the pressure recovery to 0.869.

2. The movable-cone diffuser having a 30° cone gave a maximum total-pressure recovery of 0.891 at a maximum total contraction ratio of 1.351, the theoretical isentropic contraction ratio being 1.495. With perforations at the throat of the diffuser that accomplished a partial boundary-layer removal and stabilized the normal shock, a pressure recovery of 0.933 was obtained at a total contraction ratio of 1.384.

Flight Propulsion Research Laboratory,
National Advisory Committee for Aeronautics,
Cleveland, Ohio.

REFERENCES

1. Ferri, Antonio, and Nucci, Louis M.: Preliminary Investigation of a New Type of Supersonic Inlet. NACA RM No. L6J31, 1946.

2. Kantrowitz, Arthur, and Donaldson, Coleman duP.: Preliminary Investigation of Supersonic Diffusers. NACA ACR No. L5D20, 1945.

3. Wyatt, DeMarquis D., and Hunczak, Henry R.: An Investigation of Convergent-Divergent Diffusers at Mach Number 1.85. NACA RM No. E6K21, 1946.

4. Oswatitsch, Kl.: Pressure Recovery for Missiles with Reaction Propulsion at High Supersonic Speeds (The Efficiency of Shock Diffusers). NACA TM No. 1140, 1947.

5. Oswatitsch, Kl, and Böhm, H.: Luftkräfte und Strömungsvorgänge bei angetriebenen Geschossen. Bericht Nr. 1010, Nr. 1010/2, Forschungen und Entwicklungen des Heereswaffenamtes, Kaiser Wilhelm-Inst. f. Strömungsforschung, Göttingen, Aug., Oct. 1944. (Air Forces and Flow Phenomena on Propelled Projectiles. Trans. by Douglas Aircraft Co., Inc., Feb. 14, 1946.)

6. Moeckel, W. E., Connors, J. F., and Schroeder, A. H.: Investigation of Shock Diffusers at Mach Number 1.85. I - Projecting Single-Shock Cones. NACA RM No. E6K27, 1946.

7. Moeckel, W. E., Connors, J. F., and Schroeder, A. H.: Investigation of Shock Diffusers at Mach Number 1.85. II - Projecting Double-Shock Cones. NACA RM No. E6L13, 1947.

8. Evvard, John C., and Blakey, John W.: The Use of Perforated Inlets for Efficient Supersonic Diffusion. NACA RM No. E7C26, 1947.

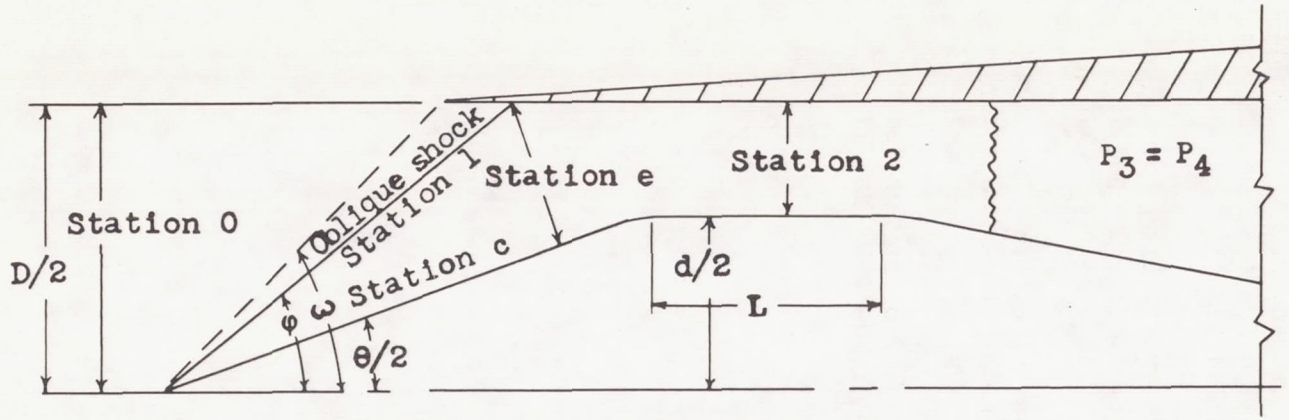

(a) Stationary-cone configuration.

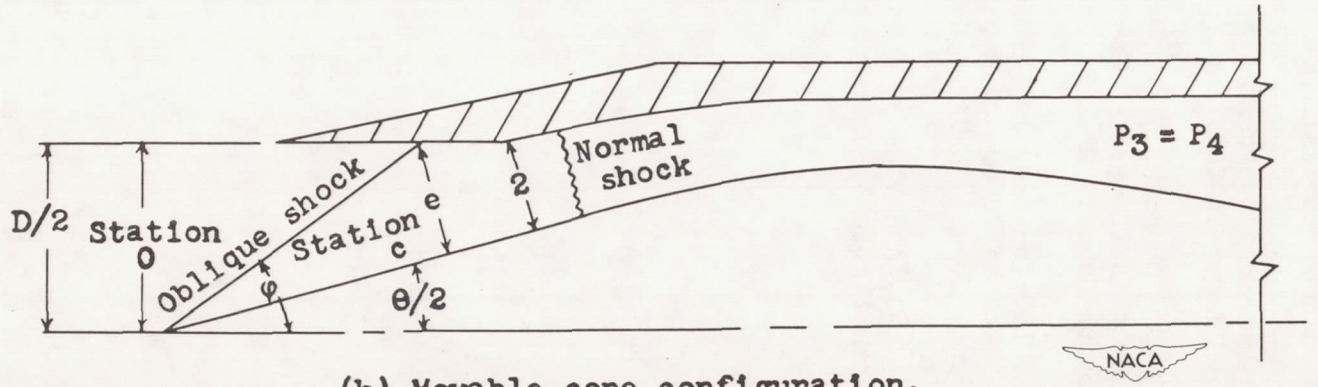

(b) Movable-cone configuration.

Figure 1. – Schematic drawing of shock-diffuser inlets with notation used.

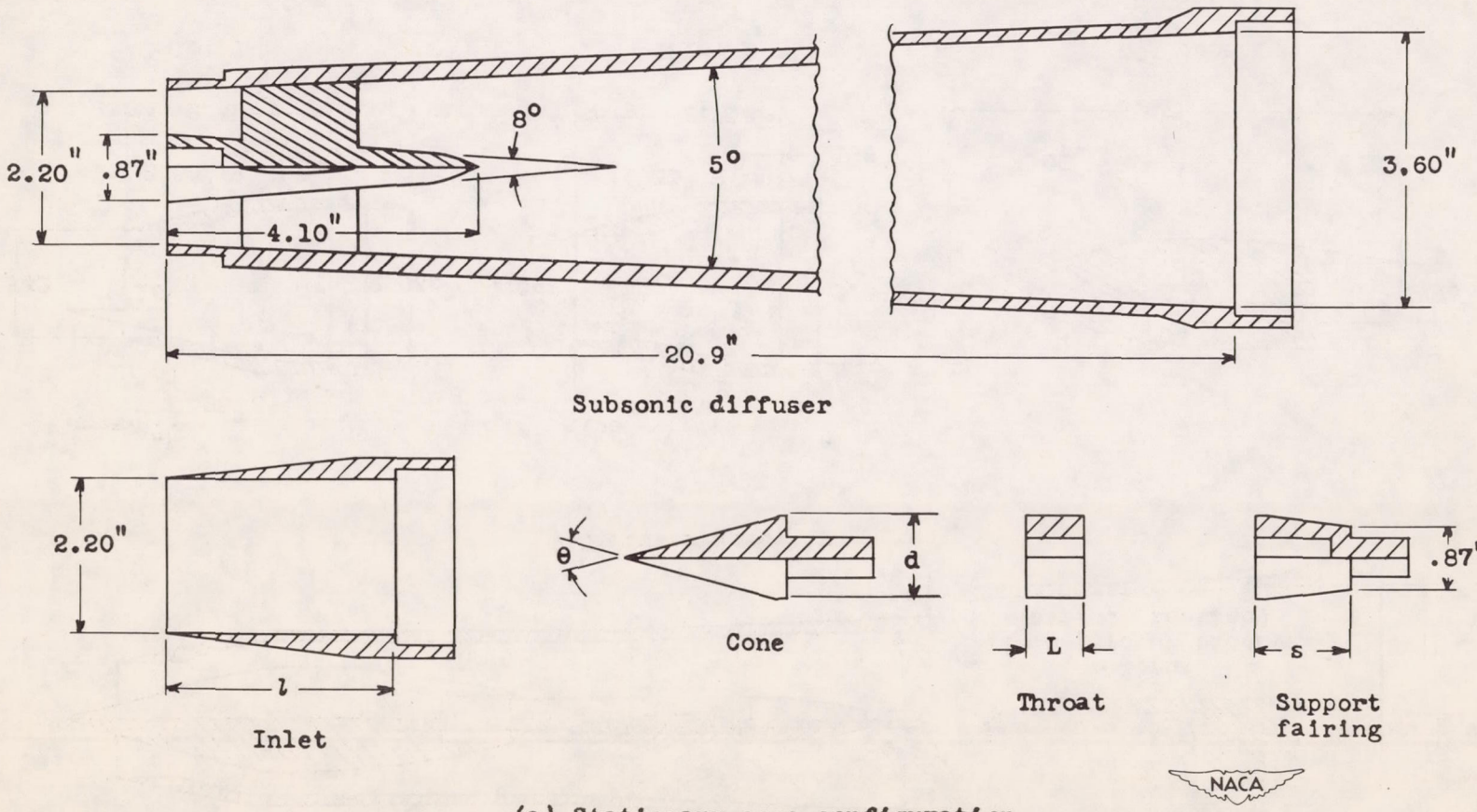

(a) Stationary-cone configuration.

Figure 2. - Experimental model.

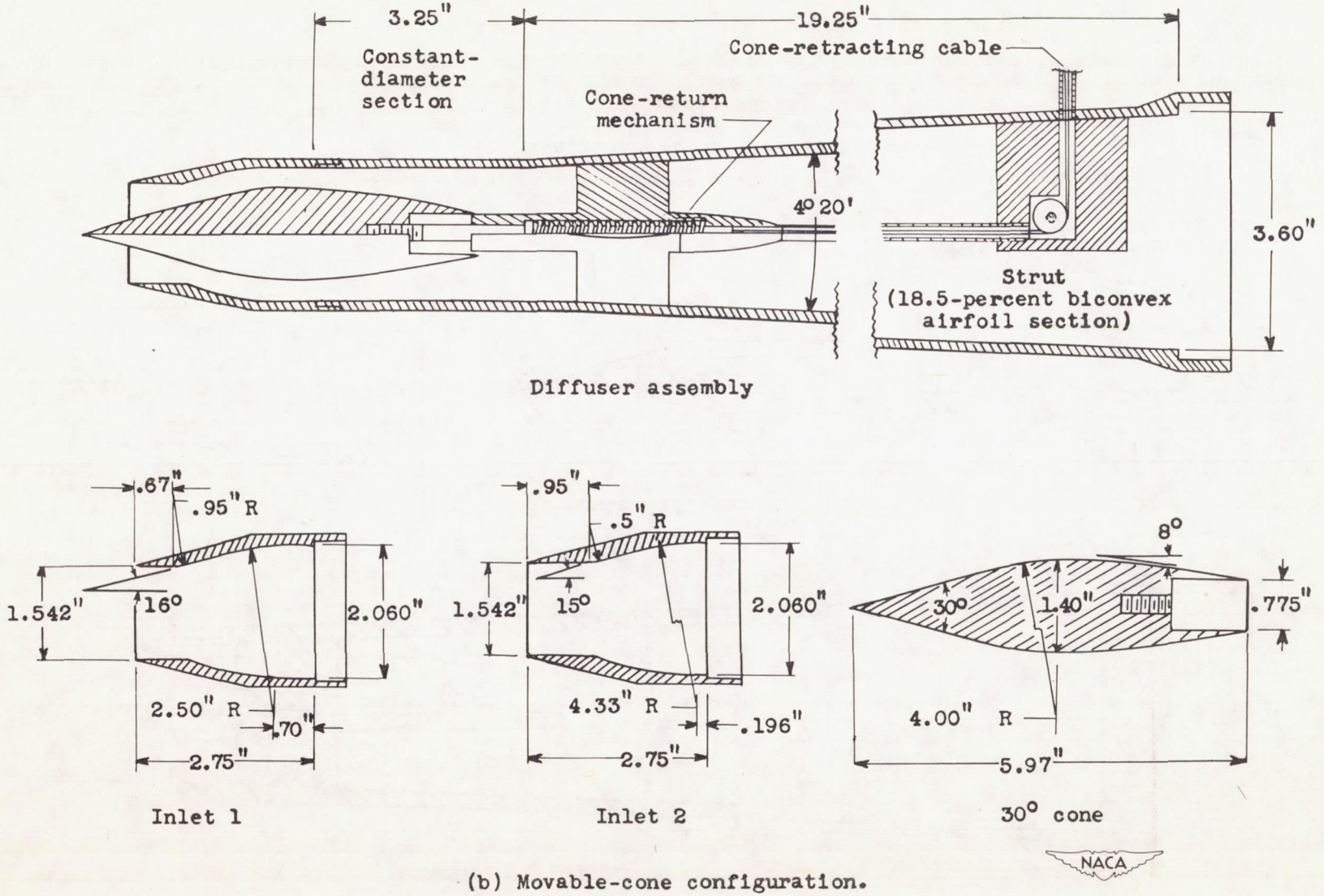

(b) Movable-cone configuration.

Figure 2. - Continued. Experimental model.

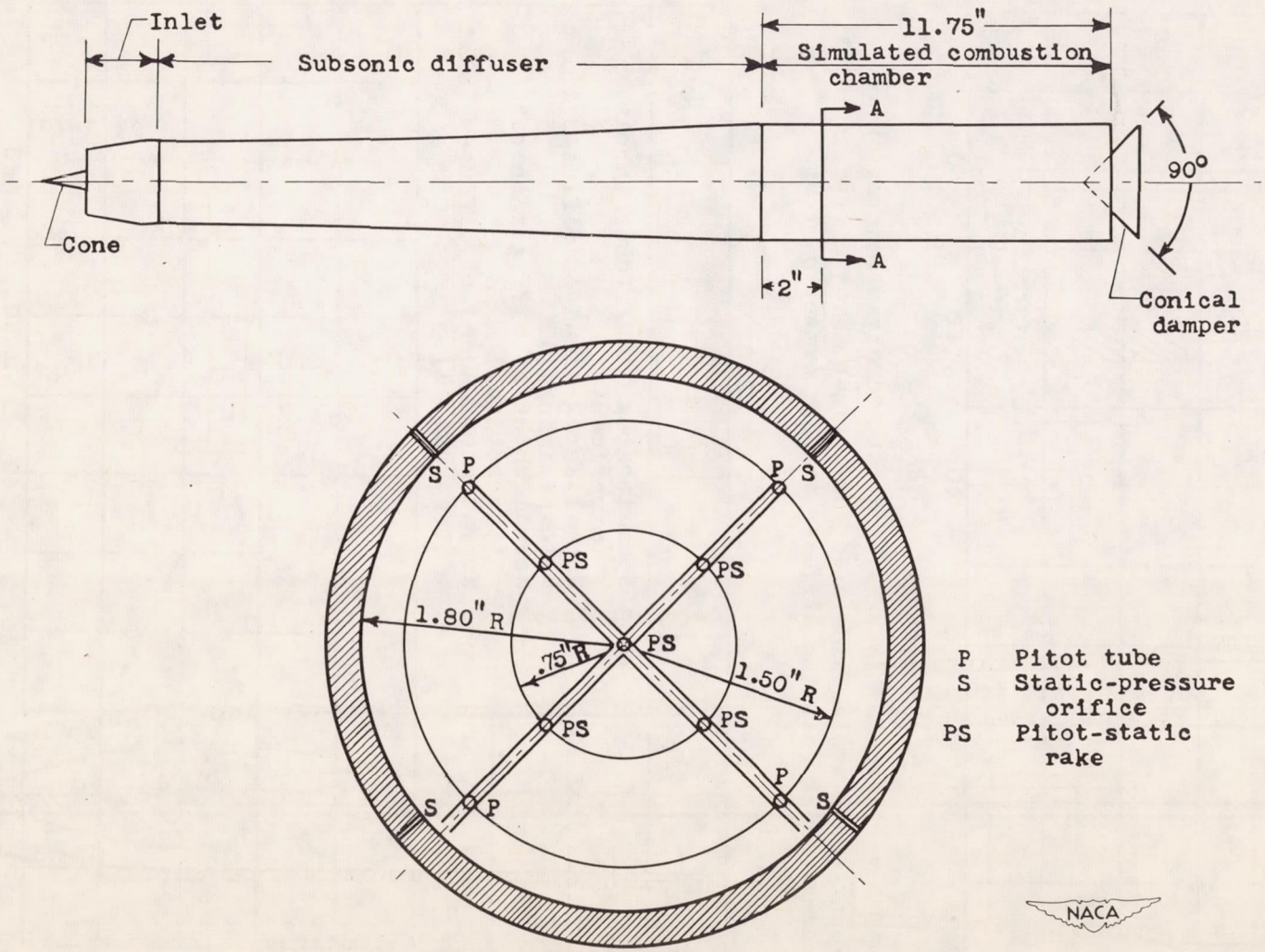

(c) Schematic drawing of model assembly showing pressure instrumentation.

Figure 2. - Concluded. Experimental model.

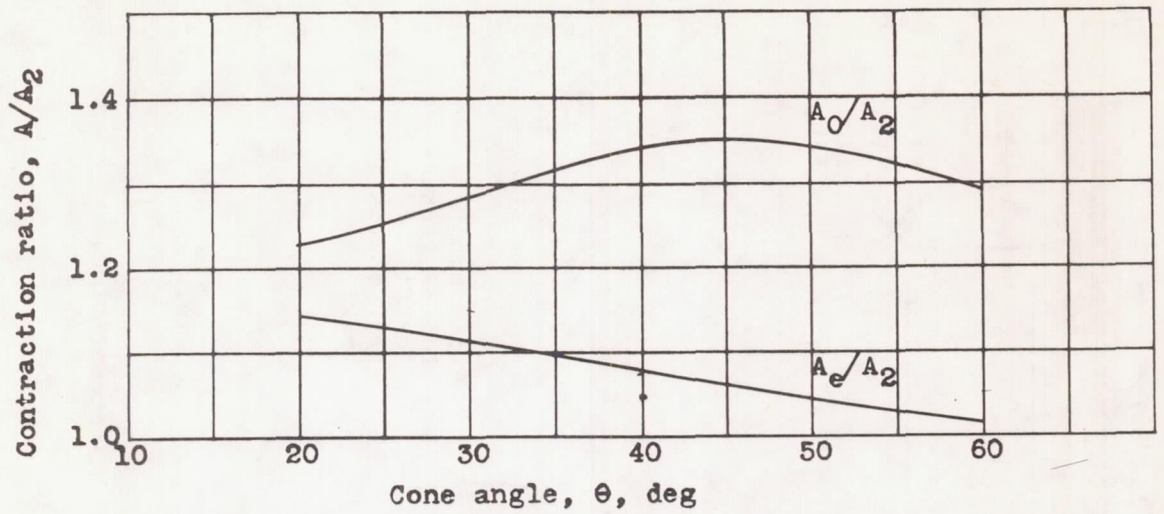

Figure 3. - Variation of internal and total contraction ratios with stationary-cone angle calculated for oblique shock at lip of inlet and normal shock entering diffuser at Mach number of 1.85.

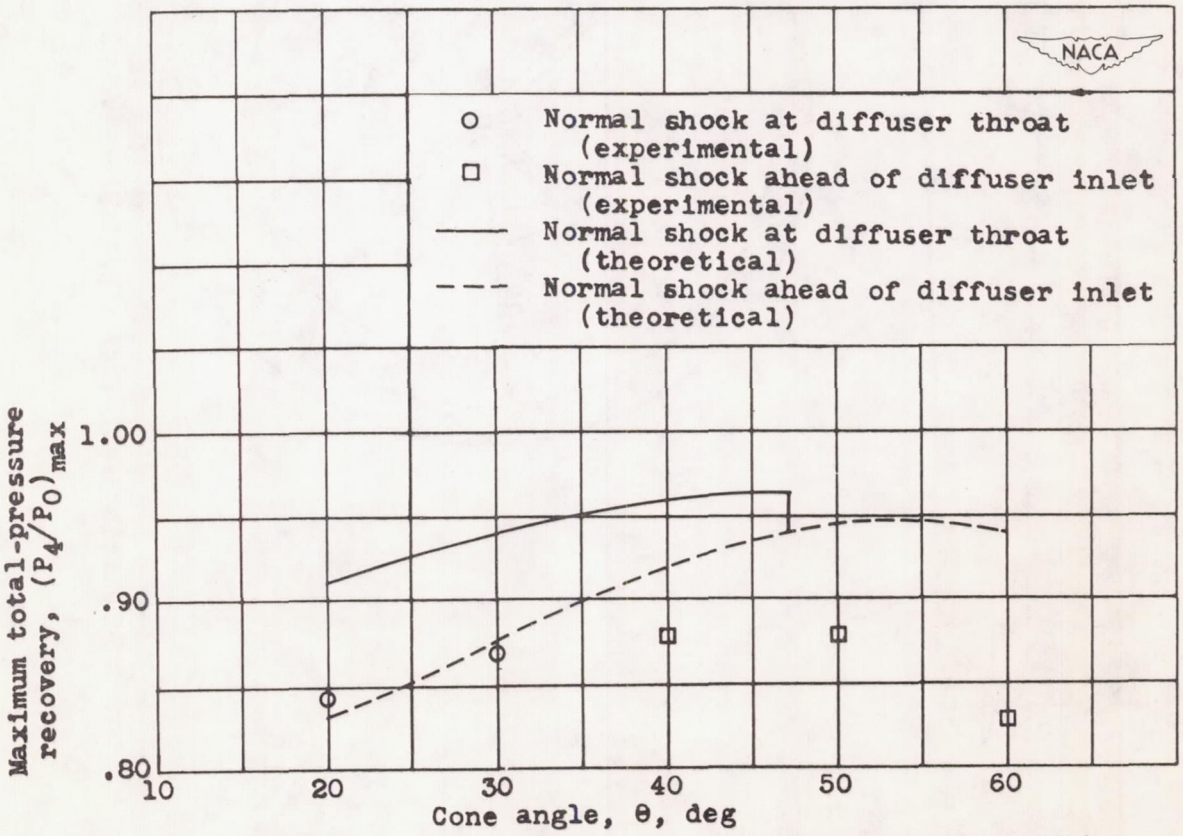

Figure 4. - Variation of maximum total-pressure recovery with stationary-cone angle for two possible shock configurations at Mach number of 1.85.

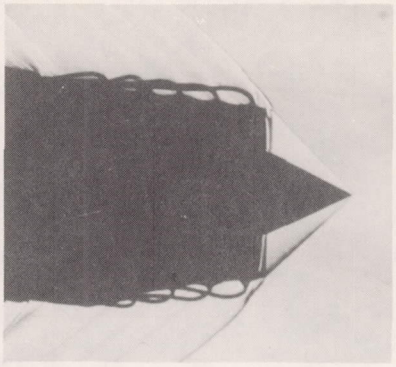

(a) 50° cone; α, 0°; P_4/P_0, 0.407; A_4/A_0, 1.880.

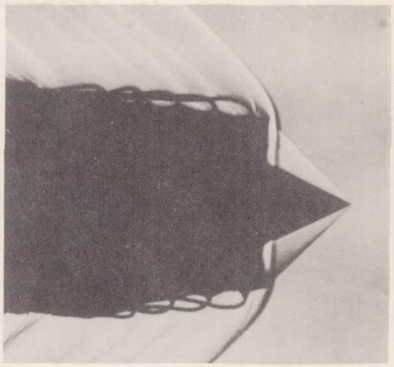

(b) 50° cone; α, 0°; P_4/P_0, 0.879; A_4/A_0, 0.755.

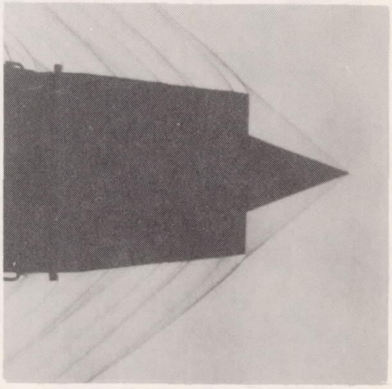

(c) 40° cone; α, 0°; P_4/P_0, 0.405; A_4/A_0, 1.900.

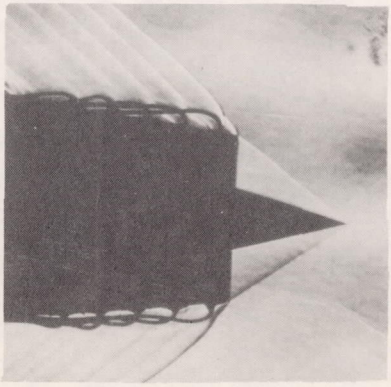

(d) 30° cone; α, 0°; P_4/P_0, 0.859; A_4/A_0, 0.870.

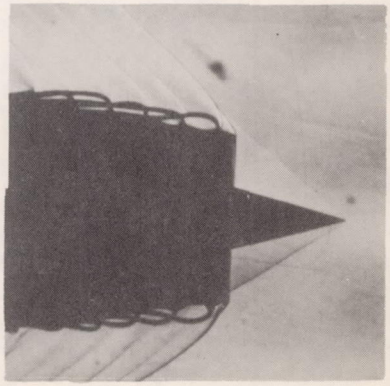

(e) 30° cone; α, 5°; P_4/P_0, 0.838; A_4/A_0, 0.890.

NACA
C-19995
11-14-47

Figure 5. - Typical flow patterns for stationary-cone configuration at Mach number of 1.85.

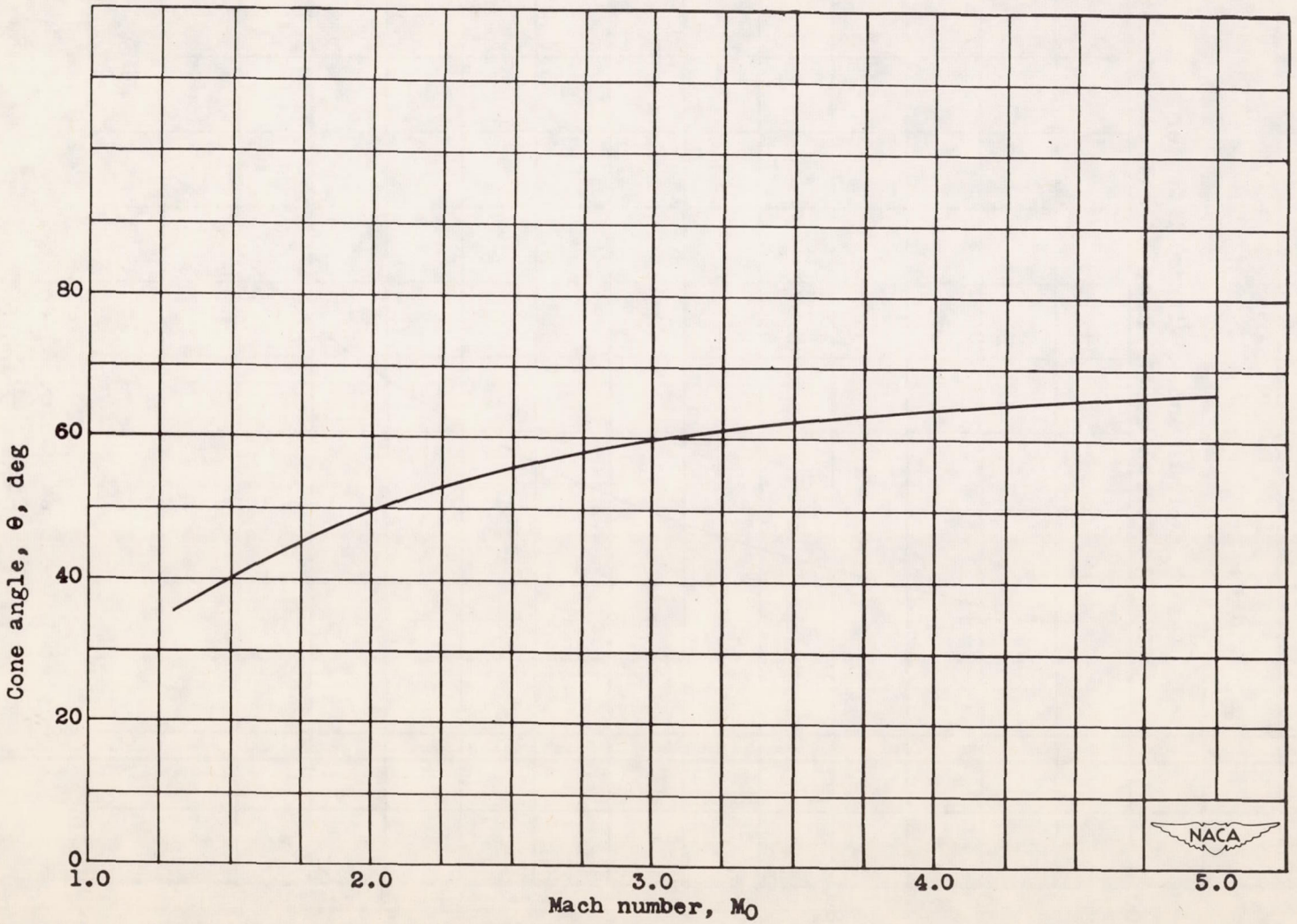

Figure 6. – Relation between design Mach number and limiting cone angle for cylindrical inlet at angle of attack of 0°.

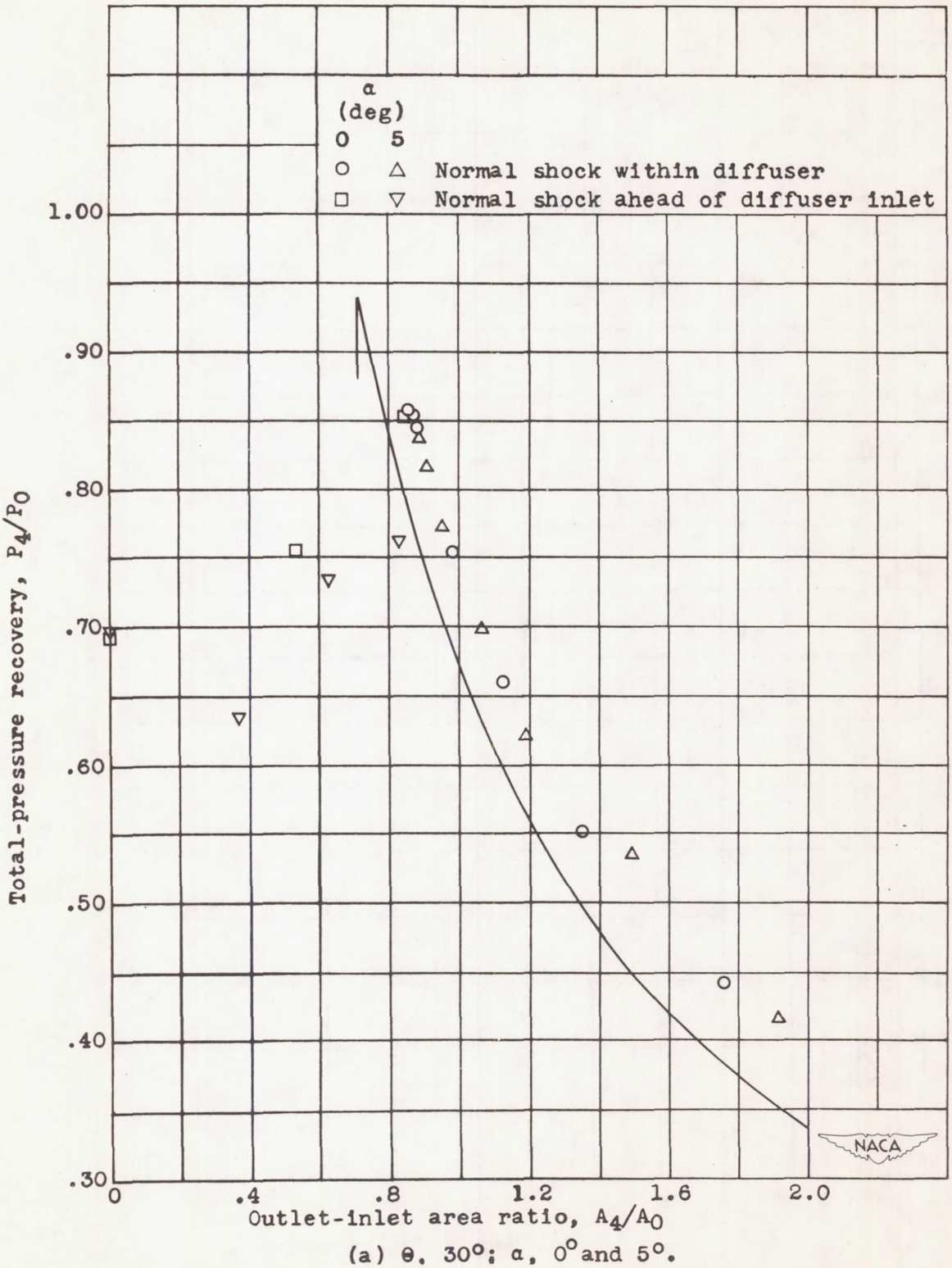

(a) θ, 30°; α, 0° and 5°.

Figure 7. - Relation between total-pressure recovery and outlet-inlet area ratio for two stationary cones at Mach number of 1.85, ω/φ of 1, and L/D of 0.29

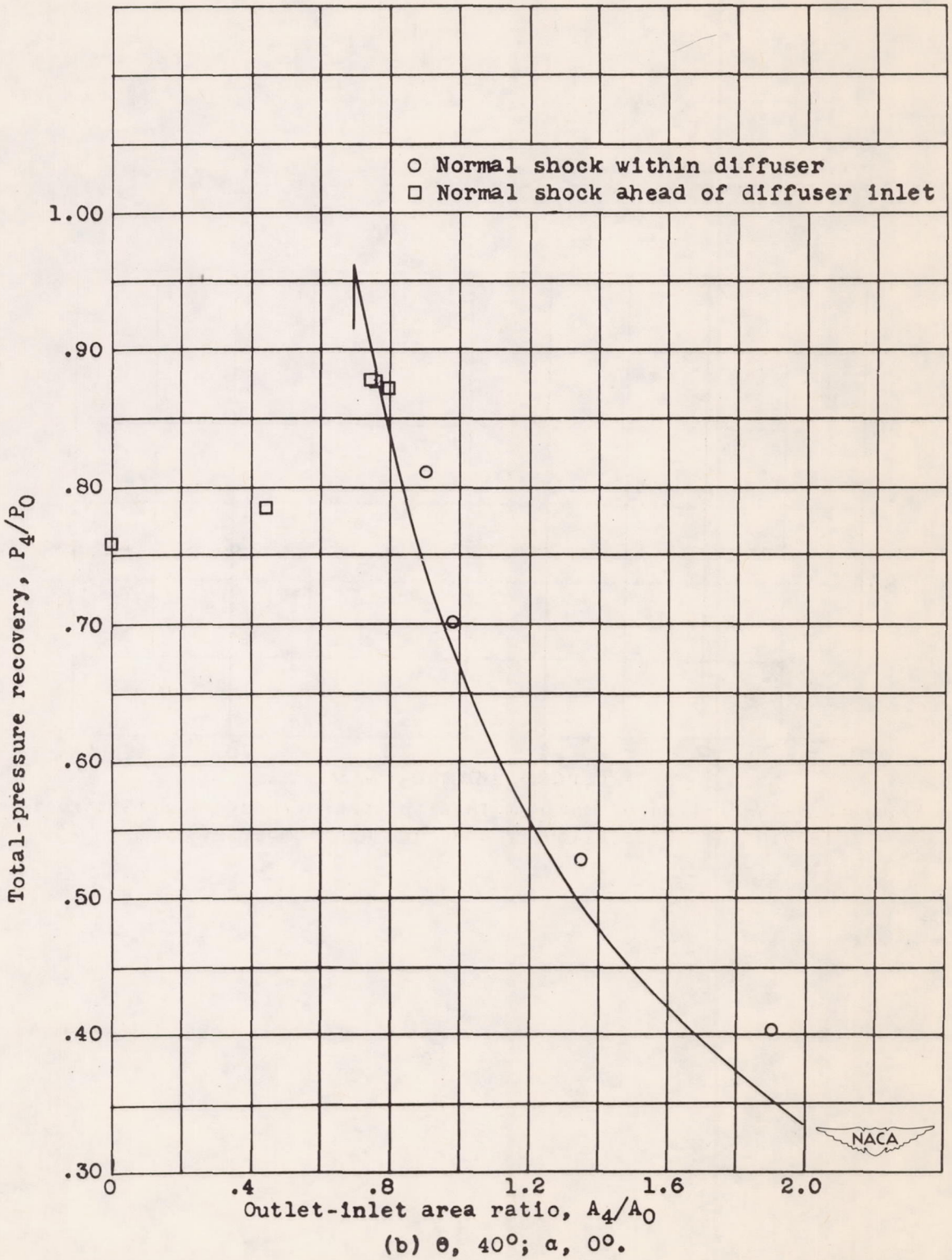

(b) θ, 40°; α, 0°.

Figure 7. - Concluded. Relation between total-pressure recovery and outlet-inlet area ratio for two stationary cones at Mach number of 1.85, ω/φ of 1, and L/D of 0.29.

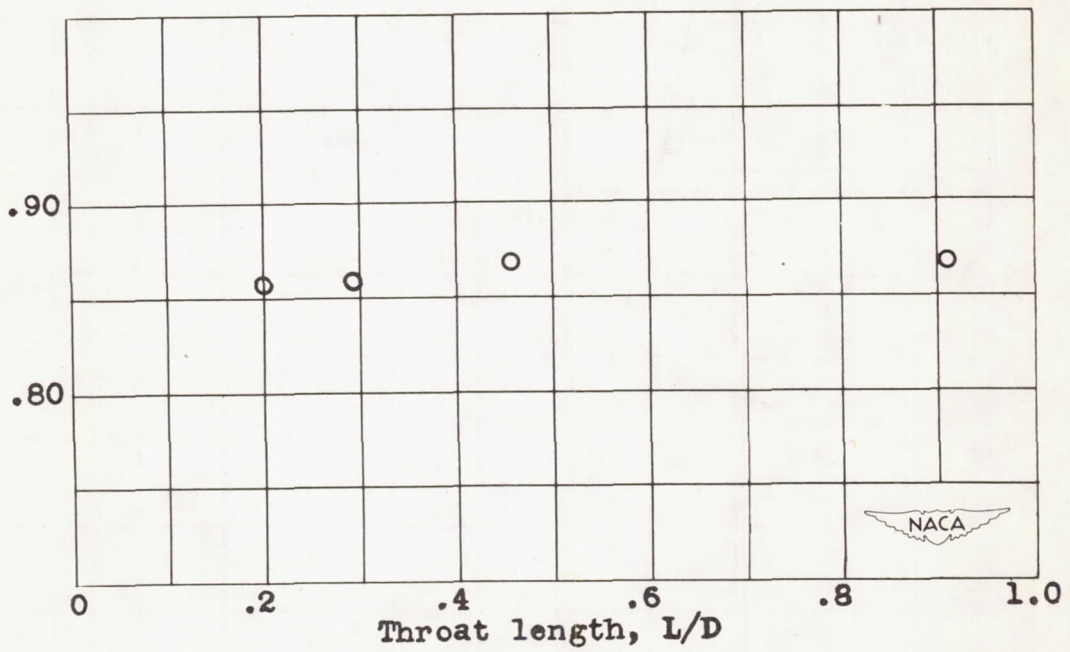

Figure 8. – Variation of maximum total-pressure recovery with throat length for 30° stationary cone at Mach number of 1.85.

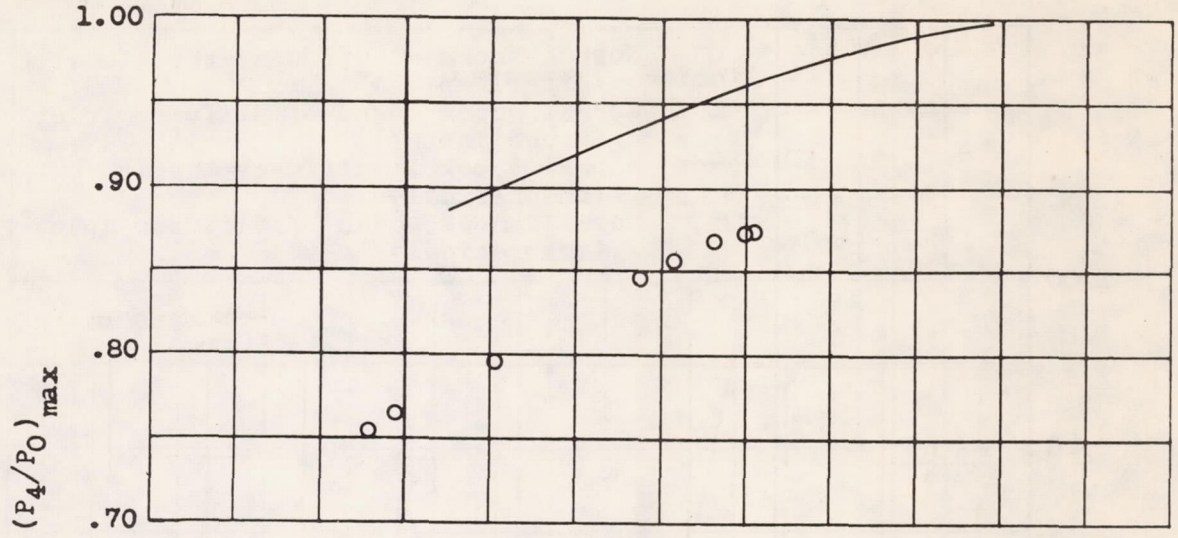

(a) Inlet 1.

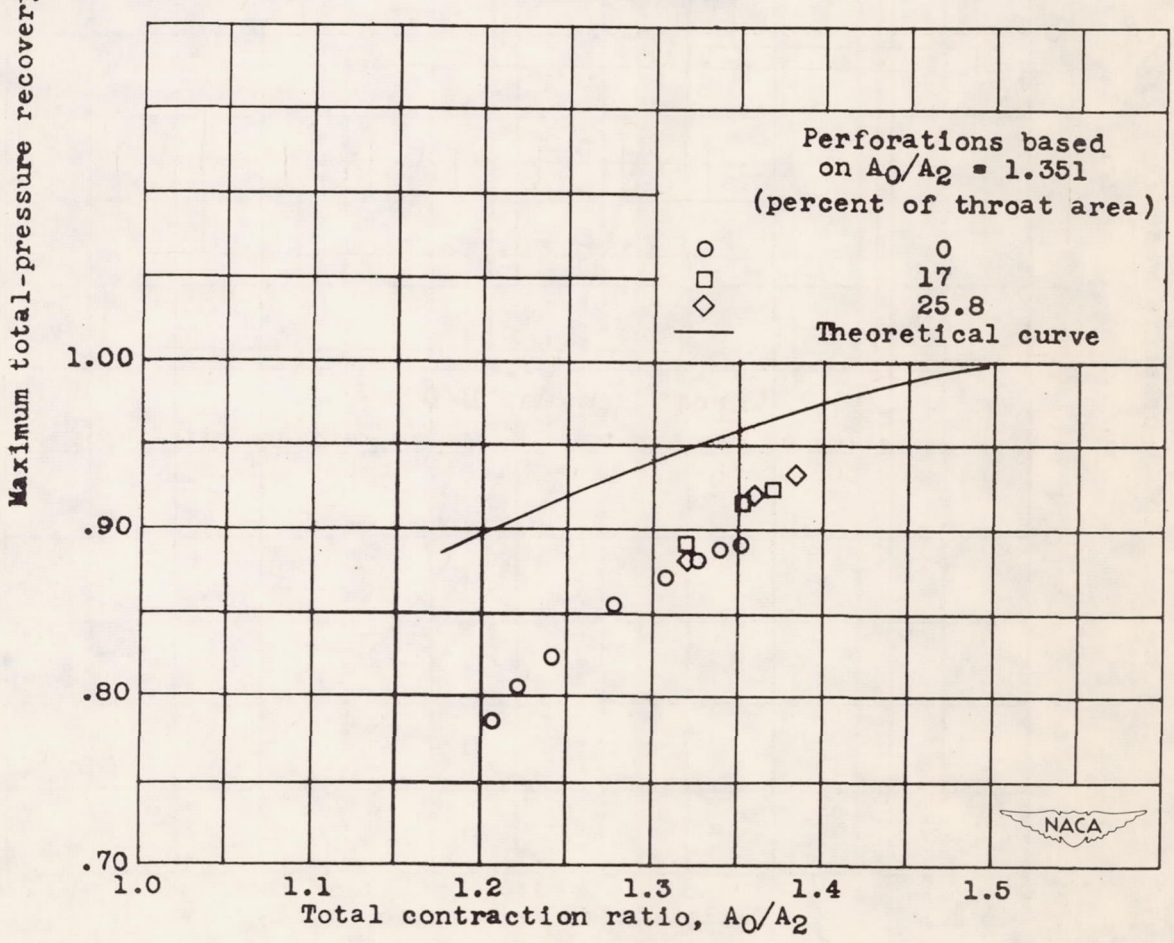

(b) Inlet 2.

Figure 9. - Relation between maximum total-pressure recovery and total contraction ratio for movable-cone configuration at angle of attack of 0° and Mach number of 1.85.

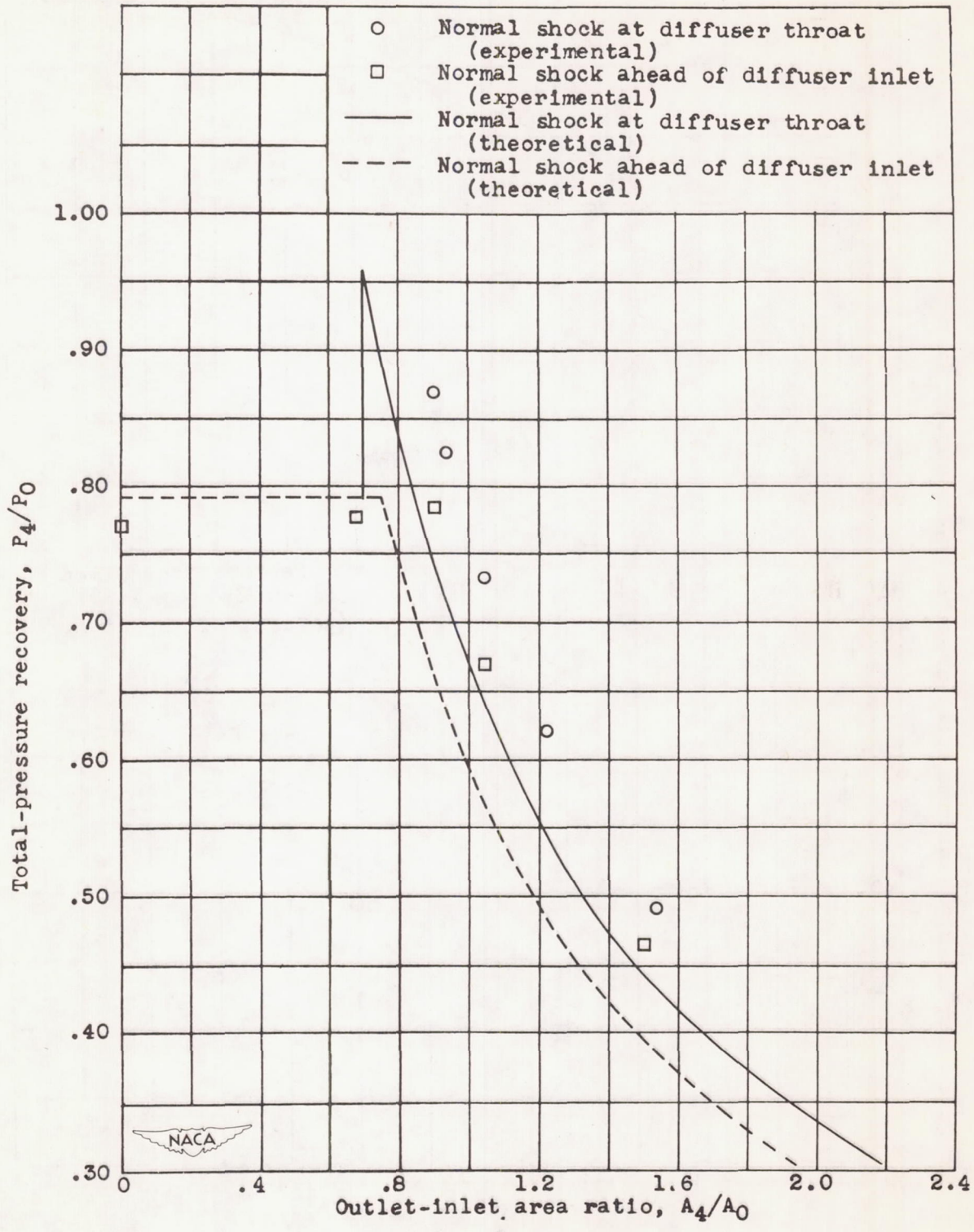

(a) A_0/A_2, 1.337.

Figure 10. - Relation between total-pressure recovery and outlet-inlet area ratio for movable-cone configuration with inlet I at angle of attack of 0° and Mach number of 1.85.

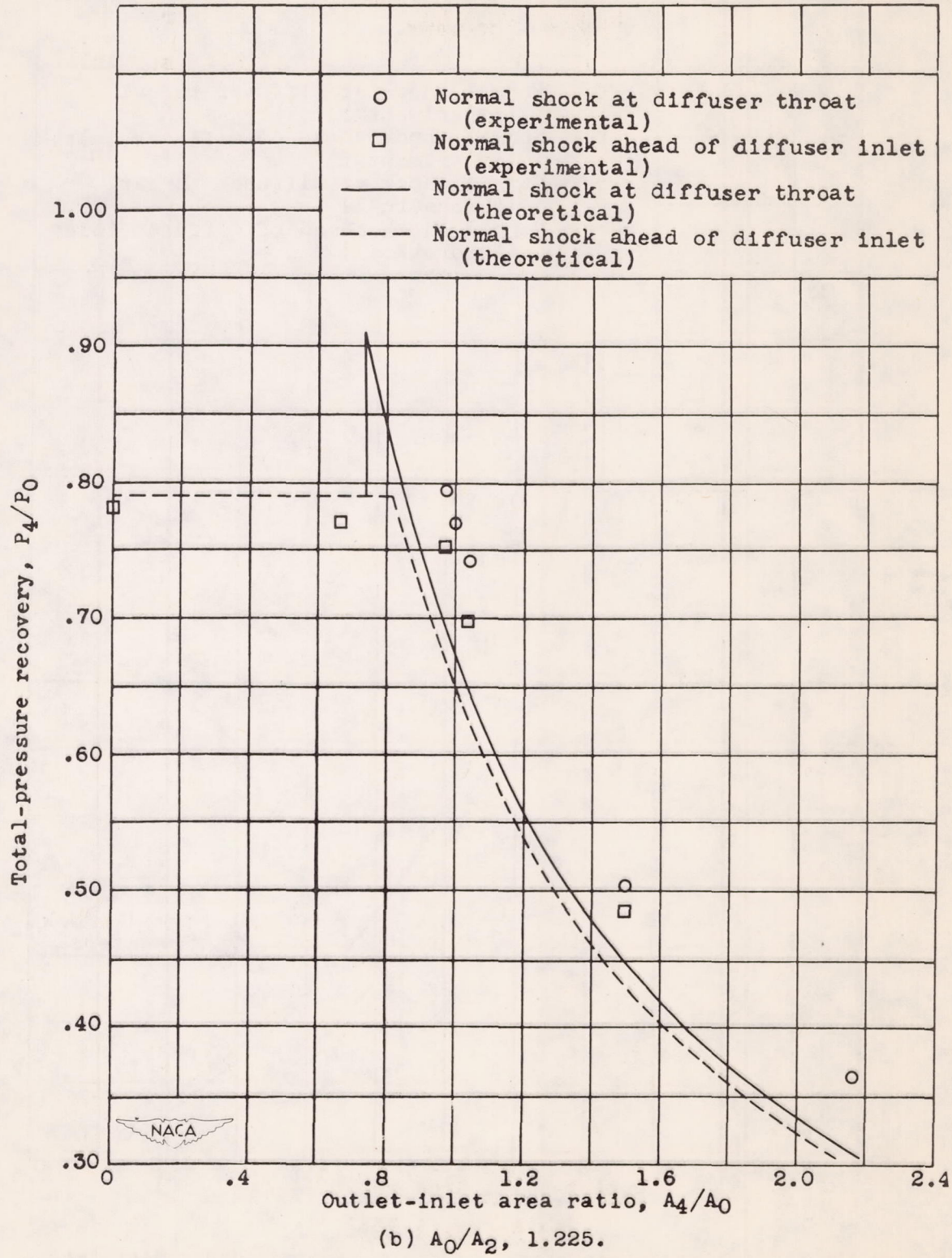

(b) A_0/A_2, 1.225.

Figure 10. - Continued. Relation between total-pressure recovery and outlet-inlet area ratio for movable-cone configuration with inlet I at angle of attack of 0° and Mach number of 1.85.

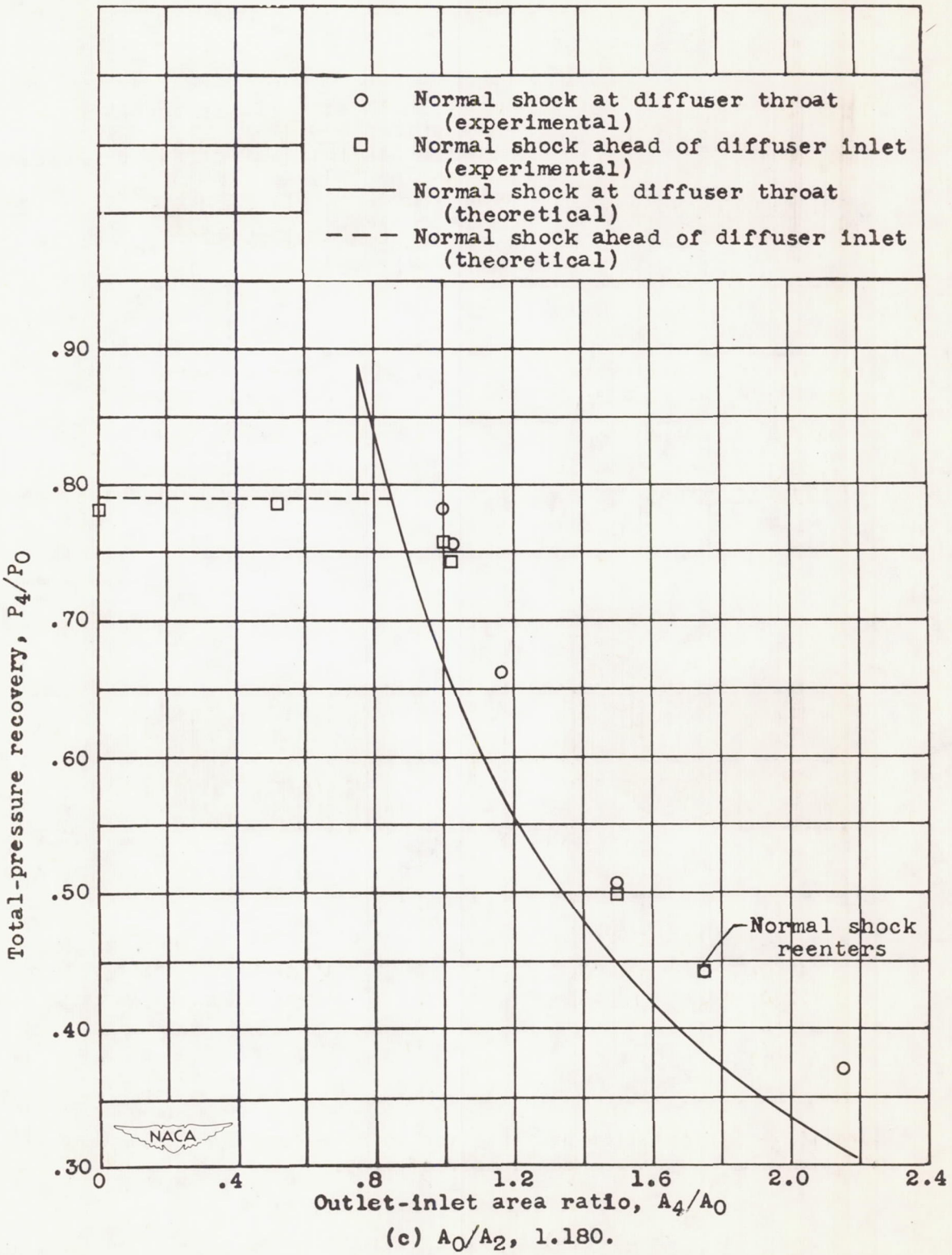

(c) A_0/A_2, 1.180.

Figure 10. - Concluded. Relation between total-pressure recovery and outlet-inlet area ratio for movable-cone configuration with inlet I at angle of attack of 0° and Mach number of 1.85.

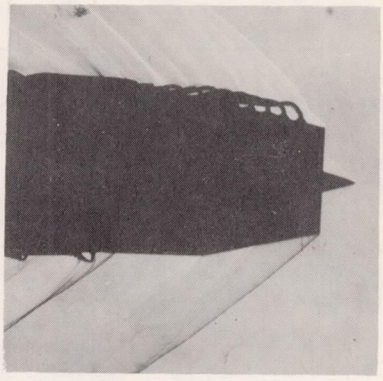

(a) Inlet 2 (perforated); α, 0°; P_4/P_0, 0.933; A_4/A_0, 0.795; A_0/A_2, 1.384; normal shock at diffuser throat.

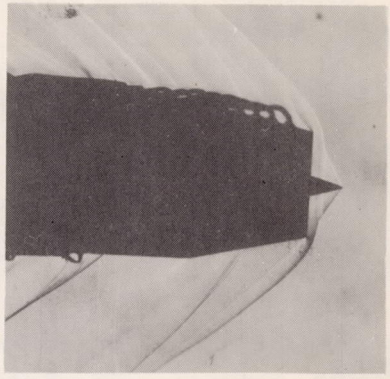

(b) Inlet 2 (perforated); α, 0°; P_4/P_0, 0.786; A_4/A_0, 0.795; A_0/A_2, 1.384; normal shock ahead of diffuser inlet.

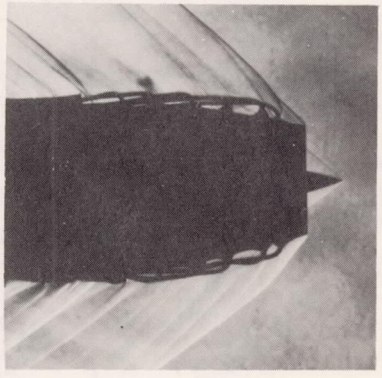

(c) Inlet 1; α, 5°; P_4/P_0, 0.613; A_4/A_0, 1.280; A_0/A_2, 1.243.

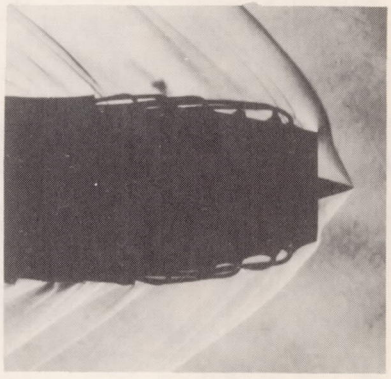

(d) Inlet 1; α, 5°; P_4/P_0, 0.785; A_4/A_0, 0.930; A_0/A_2, 1.243.

NACA
C-19996
11-14-47

Figure 11. - Typical flow patterns for movable-cone configurations at Mach number of 1.85.